

Modeling and Simulation of Thermal Behaviour and Clad Geometry Evaluation during Laser Cladding

Vikas Diwakar, Ashwani Sharma, Abhimanyu Chaudhari, Mohd Zaheer Khan Yusufzai and Meghanshu Vashista*

Department of Mechanical Engineering, Indian Institute of Technology (BHU) Varanasi, Uttar Pradesh, India

*Correspondence to:

Meghanshu Vashista
Department of Mechanical Engineering,
Indian Institute of Technology (BHU),
Varanasi, Uttar Pradesh, India.
E-mail: mvashista.mec@iitbhu.ac.in

Received: November 24, 2022

Accepted: April 19, 2023

Published: April 20, 2023

Citation: Diwakar V, Sharma A, Chaudhari A, Yusufzai MZK, Vashista M. 2023. Modeling and Simulation of Thermal Behaviour and Clad Geometry Evaluation during Laser Cladding. *NanoWorld J* 9(S1): S380-S384.

Copyright: © 2023 Diwakar et al. This is an Open Access article distributed under the terms of the Creative Commons Attribution 4.0 International License (CCBY) (<http://creativecommons.org/licenses/by/4.0/>) which permits commercial use, including reproduction, adaptation, and distribution of the article provided the original author and source are credited.

Published by United Scientific Group

Abstract

It is very important to get the desired clad geometry characteristics and quality during the laser cladding. The thermal behaviour and clad geometry evolution of Inconel 718 during laser cladding (LC) have been studied using an enhanced three-dimensional (3-D) finite element model which includes attenuation of the laser heat flux due to the convection as well as surface to ambient radiation. The cladding layer formation process is simulated and by applying the temperature-based decision-making approach to evaluate the cladding geometry which is very important to get high quality of the clad layers on the substrate. During the simulation, observed that more heat is transferred into to the substrate at the higher laser power which results more dilution percentage and at the same time cross sectional view of the clad powder showed higher temperature distribution when move downward from the surface of the substrate. With increasing laser power, the clad width, penetration depth reference to the surface and clad width increases at constant scanning speed. The dilution can be minimized by varying the scanning speed and laser power simultaneously.

Keywords

Laser cladding, Thermal behaviour, Clad geometry

Introduction

A wide range of industries, which includes tools and machinery manufacturing, marine, aerospace, and automotive, have become increasingly interested in laser cladding in recent years. Various coating materials are used in LC which are responsible for enhancing the surface properties of the substrate [1, 2]. Due to the sufficient amount of heat available for melting the powder material and the substrate surface during the laser cladding, as a result metallurgical bond is formed. For harsh working environments, the protective layer increases the substrate's corrosion resistance and wear resistance. A laser cladding coating performs better than conventional coatings because of fast heating, melting, and cooling of the melt pool. A high concentrated laser heat source is used to melt the powder or the clad material to make a metallurgical bond with the substrate. Coaxial powder systems [3], preplaced powder systems [4], off-axis powder systems [5], and wire feeding systems [6] are classified based on the powder or fibre feeding mechanism. The coaxial powder system and the preplaced powder mechanism are the two most prevalent LC mechanisms. There are a few differences between preplaced powder beds and powder feedings. In the preplaced feeding method, there no complicated system is required to feed the powder. This method is an effective way to apply coatings to substrates without requiring a complex powder feeding system. It has a few advantages over powder blowing, since powder blowing requires a larger particle size and powder flowability. The powder preplaced system has some advantage over powder blowing method in the LC. Powder blowing

may not be suitable for some mixed metal powders due to particle size differences and powder flowability. Compared to the preplaced, there is no special requirement needed to place the powder on the substrate. As a result, more variety of the powder material is available for the preplaced powder feeding mechanism compared to the cladding with blown powder.

Meng et al. [7] used the preplaced method to analyse the microstructure and morphology of the Ni base composite on Ti-6Al-4V substrate and observed that at low laser energy a free from crack and pores clad layer are formed. Ng et al. [8] used the Mo as cladding powder on the copper to enhance the wear resistance in the electrical contacts. Also, in their analysis they used the preplaced powder mechanism because high reflectivity of the Cu can be eliminated and absorb more energy easily. Tseng et al. [9] done a simulation study in which temperature distribution and clad bead profile is explored. Cobalt powder is preplaced on a steel substrate and observed that CO₂ laser produced a deeper melt pool compared to the Nd-YAG laser. Thawari et al. [10] considered the preplaced approach to analyse the temperature distribution and stress on the melt pool of the clad Inconel 718 on the SS316 substrate and in their analysis, they did not consider the heat attenuation due to the convection and surface to ambient which causes less clarity about the temperature distribution in the melt pool.

A proper manufacturing process for laser cladding should be studied due to the high processing temperature and superfast changes in materials states and measuring thermal behaviour with help of experiments makes it very difficult and challenging. In order to resolve this type of problem, numerical modeling and simulation is used to assess the thermal behaviour and clad geometry characteristics of the clad material on the substrate. It was possible to solve the laser cladding problem numerically, it is not only interpreting the results of the experiment, but also to show the evolution of the experiment continuously and dynamically to facilitate the understanding of the overall process based on numerical simulation. In this paper, using the preplaced method for placing the powder of Inconel 718 on the SS316 substrate and a FEM is developed to analyse the thermal behaviour and the clad geometry characteristics of Inconel 718 alloy and SS316 substrate during laser cladding. In the model, a modified 3-D FEM is used which considered the heat losses due to the convection as well as radiation both.

Development of Thermal Model

FEM-based thermal model is developed which is dependent on the time to assess the clad geometry characteristics and distribution pattern and values of the temperature in the melt pool during the cladding of the Inconel 718 powder on the SS316 substrate. The spatial dimension of the SS316 substrate were selected as 120 x 65 x 8 mm³ and 0.3 mm thickness of the Inconel 718 powder is placed on the substrate to perform the FEM-based simulation using standard COMSOL Multiphysics to assess the distribution of the temperature in the melt pool of the powder when applied the heat source which is shown in the figure 1. The compositional details of

both materials are mentioned in the table 1. 3-D laser heat sources are used which is moving over the preplaced powder to analyse the thermal and clad geometry behaviour during the simulation and the mathematical expression [10] of the heat flux is shown in equation 1.

$$Q_g = \frac{2AP}{\pi R_s^2} \exp \left\{ -2 \left\{ \left(\frac{r_x^2}{R_s^2} \right) + \left(\frac{r_y^2}{R_s^2} \right) \right\} \right\} \quad (1)$$

Where, A is absorptivity, P is the laser power, R_s is beam radius, r_x and r_y are distance in the radial and in-depth direction, respectively. The constant and variables process parameters are mentioned in the table 2 which is directly extracted from the 3-D geometry where x₀, y₀ and z₀ are the initial position of the laser beam.

Assumption for the thermal model

The melt pool geometry is considered as an elliptical cross section and width is considered equal to the diameter of the laser beam.

- Material loss due to evaporation is neglected.
- Heat losses due to the convection and radiation are considered.
- No heat is losing from the side faces of the substrate.
- Temperature dependent thermal properties of the material are considered.

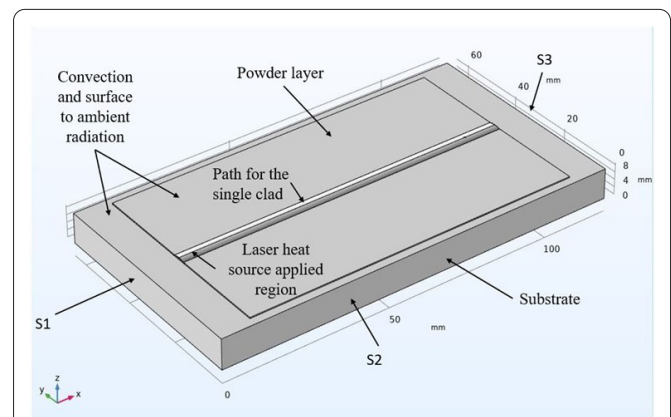


Figure 1: Geometry for thermal model.

Table 1: Chemical composition (wt%) [2].

Elements	Inconel 718	SS316
C	0.08	0.08
Cr	19	17
Cu	0.3	0.3
Fe	16.7	65
Mn	0.35	2.0
Mo	3.1	2.5
Ni	52.5	12
Si	0.35	1
Al	0.5	-
Co	1	-
Nb	5.2	-
Ti	0.9	-

Table 2: Process parameters used during simulation.

Name	Expression	Unit
P	4200 - 6200	W
x_0	10	mm
y_0	32.5	mm
z_0	8.30265	mm
f	12	mm/s
r_x	$\text{sqrt}((x - x_0 - f \cdot t)^2)$	m
r_y	$\text{sqrt}((y - y_0)^2)$	m
r_z	$\text{sqrt}((z - z_0)^2)$	m
Q_0	$Q_0 = \frac{2AP}{\pi R_s^2} \exp\left[-2\left\{\left(\frac{r_x^2}{R_s^2}\right) + \left(\frac{r_y^2}{R_s^2}\right)\right\}\right]$	W/m ²

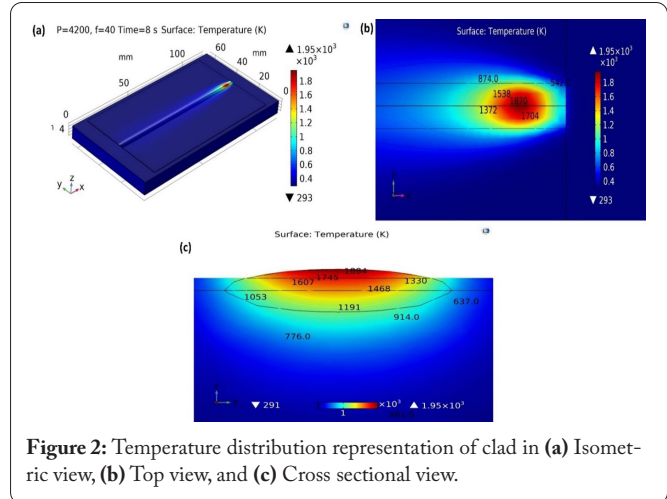


Figure 2: Temperature distribution representation of clad in (a) Isometric view, (b) Top view, and (c) Cross sectional view.

Governing equation

The transition heat transfer model in the powder and substrate are mentioned in the equation 2 which is utilized to assess the pattern of the temperature distribution and clad geometry.

$$\rho C_p \frac{\partial T}{\partial t} + \rho C_p u \cdot \nabla T + \nabla q = Q \quad (2)$$

Where, u is velocity field related to the motion of the laser beam, t is interaction time, C_p , q, ρ and T are specific heat transfer coefficient at constant pressure, volumetric heat generation, density, and temperature. The heat losses due to convection and radiation is considered on the top surface of the substrate and neighbouring powder particles which are pre-placed on the substrate and their expression are mentioned in the equation 3 and equation 4.

$$Q_c = h(T - T_{amb}) \quad (3)$$

$$Q_r = \epsilon \sigma (T_{amb}^4 - T^4) \quad (4)$$

Where, ϵ is the emissivity, T_{amb} is ambient temperature, σ is Stefan-Boltzmann constant, and h is convective heat transfer coefficient.

Results and Discussion

Thermal analysis

The laser heat source is applied on the preplaced powder and the initial position or coordinate of the laser spot is (10,32.5,10.30265) with scanning speed of the 12 mm/s. To complete a single clad on the substrate needed nearly 8.3 s. The laser power is varied from 4200 W to 6200 W and observed a direct correlation between the temperature distribution with increasing laser power. The isometric, top, and cross-sectional view of the temperature distribution is shown in figure 2. As the power increases the temperature distribution of the cladded portion is increases because of the more heat addition into the melt pool. From the figure 2b observed that as move away from the centre of applying heat flux observed that, in radial direction the magnitude of temperature get reduces and the variation of the temperature with distance along the

depth from the centre of the laser beam shown in the figure 3a which indicate that as move downward from the top surface, the temperature get reduces. The correlation between the laser power and temperature distribution is shown in figure 3b.

Clad geometry evolution

Under the influence of laser light, the cladding powder melts and solidifies fast on the substrate surface. To obtain a uniform clad geometry is very important at the LC process which is directly influence the mechanical properties and quality of the cladded material on the substrate [1]. Many of the experiments was performed by the various researcher to obtain a high quality of the clad geometry and optimum dilu-

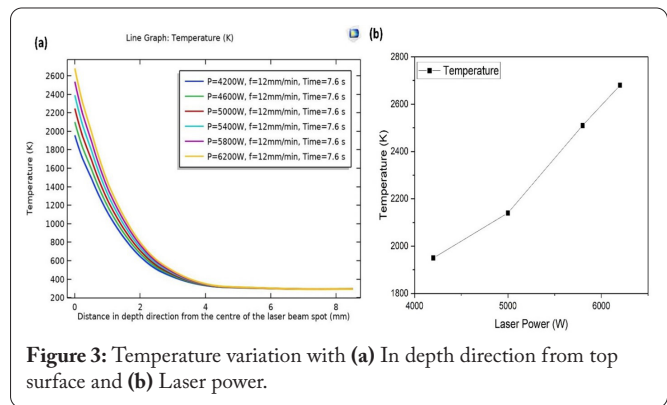


Figure 3: Temperature variation with (a) In depth direction from top surface and (b) Laser power.

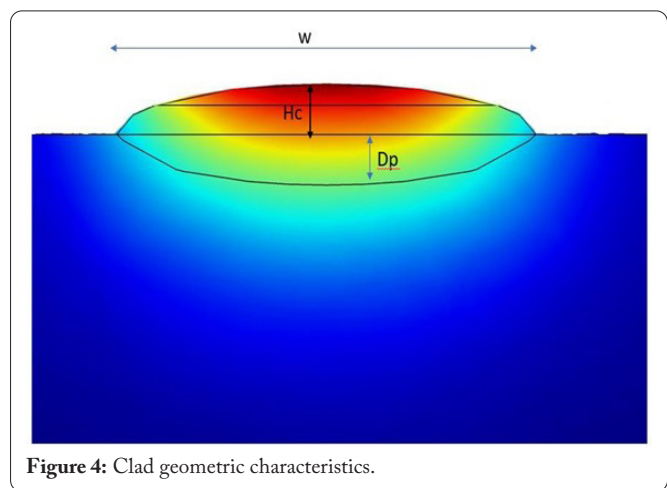


Figure 4: Clad geometric characteristics.

tion with different type of the high corrosive and temperature resistant material for cladding over the substrate. In this paper an approach is made to estimate the clad geometry characteristics which give a clear idea about the quality and dilution of the cladded powder on the substrate. The description of the clad geometry is shown in the figure 5 which included the information about the clad height (Hc), weld width (w), and penetration depth reference to the surface (Dp).

The processing parameter i.e., laser power and scanning speed influence the clad geometry and the effect of the clad geometrical dimension and dilution is extracted from the simulated geometry which is listed in the table 2. In the analysis observed that as the laser power increases the dilution rate is increases which is shown in figure 5 and it can optimize by selecting the proper scanning speed and laser power simultaneously. There is insufficient metallurgical bond form when applying the lower laser power because the temperature values is not reaching up to the melting point of the powder material as well as near the interface of the substrate and cladded layer which result, a weak bonding formed.

Model validation

To ensure the accuracy of the developed thermal and clad geometrical model, the variation of the temperature at the 3-D point with time is compared with the literature [9] by considering the same process parameters which is shown in the figure 6a. The maximum error occurred is about 5.2% with the present simulated data. Also, convergent plot is drawn between the domain elements and temperature distribution. From the convergent plot it observed that after the normal meshing which contains 29583 domain elements, 9150 boundary elements and 812 edge elements, there is no

variation of the temperature as increases the domain elements therefore normal meshing is considered during the simulation to analyse all the responses.

Conclusion

In this research, thermal behaviours and clad geometry evaluation is made which gave a clear idea about the clad geometry characteristics and temperature distribution in the weld zone of the cladded material as well as within the substrate. The direct correlation showed between the temperature variation and laser power on the melt pool. The clad geometry characteristics and temperature distribution can be controlled by selecting optimum laser power and scanning speed. The percentage of dilution observed more for higher laser power at constant scanning speed. The maximum error appeared about 5.2% for temperature distribution with the simulation time.

Acknowledgements

None.

Conflict of Interest

The authors declare no conflict of interest.

Credit Author Statement

Vikas Diwakar: Conceptualization, Modeling, Simulation, Data curation; Ashwani Sharma: Writing - review and editing; Abhimanyu Chaudhari: Writing - review and editing; Mohd Zaheer Khan Yusufzai: Writing - review and editing, Supervision; Meghanshu Vashista: Writing - review and editing, Supervision. All the authors read and approved the manuscript.

References

- Siddiqui AA, Dubey AK. 2021. Recent trends in laser cladding and surface alloying. *Opt Laser Technol* 134: 106619. <https://doi.org/10.1016/j.optlastec.2020.106619>
- Fu Y, Guo N, Zhou C, Wang G, Feng J. 2021. Investigation on in-situ laser cladding coating of the 304 stainless steel in water environment. *J Mater Process Technol* 289: 116949. <https://doi.org/10.1016/j.jmatprotec.2020.116949>
- Doubenskaia M, Kulish A, Sova A, Petrovskiy P, Smurov I. 2021. Experimental and numerical study of gas-powder flux in coaxial laser cladding nozzles of Precitec. *Surf Coatings Technol* 406: 126672. <https://doi.org/10.1016/j.surfcoat.2020.126672>
- Deng D, Li T, Huang Z, Jiang H, Yang S, et al. 2022. Multi-response optimization of laser cladding for TiC particle reinforced Fe matrix composite based on Taguchi method and grey relational analysis. *Opt Laser Technol* 153: 108259. <https://doi.org/10.1016/j.optlastec.2022.108259>
- Grohol CM, Shin YC, Frank A. 2021. Laser cladding of aluminum alloy 6061 via off-axis powder injection. *Surf Coatings Technol* 415: 127099. <https://doi.org/10.1016/j.surfcoat.2021.127099>
- Zhang Z, Kong F, Kovacevic R. 2020. Laser hot-wire cladding of Co-Cr-W metal cored wire. *Opt Lasers Eng* 128: 105998. <https://doi.org/10.1016/j.optlaseng.2019.105998>
- Meng QW, Geng L, Zhang BY. 2006. Laser cladding of Ni-base composite coatings onto Ti-6Al-4V substrates with pre-placed B₄C+Ni-CrBSi powders. *Surf Coatings Technol* 200(16-17): 4923-4928. <https://doi.org/10.1016/j.surfcoat.2005.04.059>

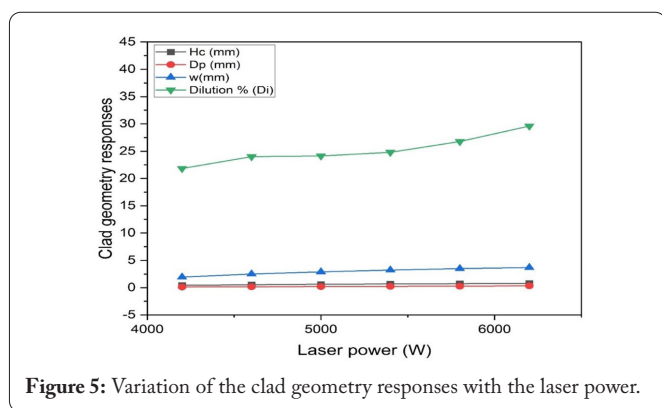


Figure 5: Variation of the clad geometry responses with the laser power.

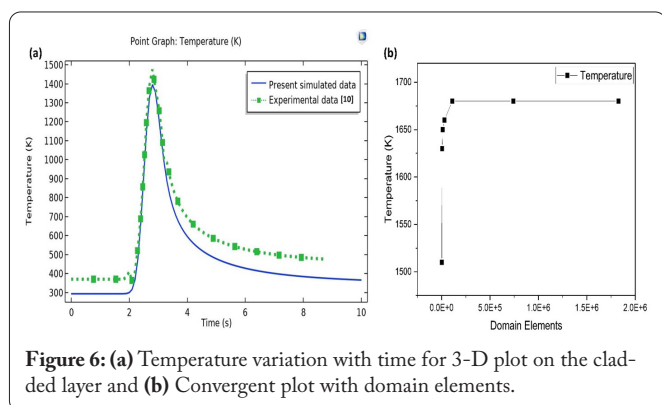


Figure 6: (a) Temperature variation with time for 3-D plot on the cladded layer and (b) Convergent plot with domain elements.

8. Ng KW, Man HC, Cheng FT, Yue TM. 2007. Laser cladding of copper with molybdenum for wear resistance enhancement in electrical contacts. *Appl Surf Sci* 253(14): 6236-6241. <https://doi.org/10.1016/j.apsusc.2007.01.086>
9. Tseng WC, Aoh JN. 2013. Simulation study on laser cladding on pre-placed powder layer with a tailored laser heat source. *Opt Laser Technol* 48: 141-152. <https://doi.org/10.1016/j.optlastec.2012.09.014>
10. Thawari N, Mhala B, Gullipalli C, Chandak A, Gupta TVK. 2021. Analysis of melt pool temperature and stresses in laser cladding of inconel 718. *AIP Conf Proc* 2341(1): 040009.